

HIGH-ANGULAR RESOLUTION OBSERVATIONS OF HD179218: EARLY STAGES OF DISK DISSIPATION?

J. Kluska¹, S. Kraus², C. L. Davies², T. Harries², M. Willson², J.D. Monnier³, A. Aarnio⁴, F. Baron⁵, R. Millan-Gabet⁶, T. ten Brummelaar⁷, X. Che³, S. Hinkley², T. Preibisch⁸, J. Sturmann⁷, L. Sturmann⁷ and Y. Touhami⁵

Abstract. Star/disk interactions have an important effect on disk evolution (e.g. photoevaporation). We present an extensive multi wavelength (visible, near- and mid-infrared) high-angular resolution observational campaign involving seven instruments (direct imaging and interferometry), on HD179218, a Herbig star surrounded by a (pre-)transitional disk. Its near-infrared circumstellar emission is 50 times larger than its theoretical dust sublimation radius making it very special amongst other Herbig stars observed by infrared interferometry. This emission has an unexpectedly high temperature (~ 1500 K) that we postulate to explain by small carbon particles super-heated by high energy photons from the central star. This points toward a scenario where the inner disk parts were accreted onto the star and the rest of the disk is being photo-evaporated by high energy stellar photons. It makes this target unique as it would be the first one to be caught in very early stages of disk dissipation.

Keywords: young stars, protoplanetary disks, transition disk, high angular resolution, interferometry, direct imaging.

1 Introduction

To understand the mechanisms of planet formation it is necessary to observe and study the place where planets form, namely the protoplanetary disks. Recent observations with direct imaging or radio interferometry revealed various structures of protoplanetary disks such as warps, spirals or gaps (e.g. Stolker et al. 2017; Andrews et al. 2018; Avenhaus et al. 2018) that are signs of disk evolution. After few million years the disks likely dissipate via photo-evaporation from inside out (e.g. Alexander et al. 2014, and references therein). The disk dissipation has a strong impact on planet formation. To constrain the disk evolution and dissipation processes it is needed to study the inner regions in detail. It was first done by studying the infrared excess in the spectral energy distributions (SED) of young stars as the near infrared emission was interpreted as coming from the dust located within the first astronomical units from the star. The intermediate-mass young stars, called the Herbig stars (Herbig 1960), were classified into two groups based on the shape of the infrared excess (Meeus et al. 2001). Group I sources have a black-body-like excess around $10\mu\text{m}$ whereas the infrared excess of group II targets can be reproduced with a power-law. It was first interpreted that group I objects are flared disks whereas group II are flat disks and that the evolution sequence goes from group I to group II objects. Nevertheless, resolved observations have shown that group I disks are rather transition disks with gaps or holes and that the evolution sequence goes the other way around (Maaskant et al. 2013; Menu et al. 2015).

¹ Instituut voor Sterrenkunde (IvS), KU Leuven, Celestijnenlaan 200D, 3001, Leuven, Belgium.

² Astrophysics Group, School of Physics and Astronomy, University of Exeter, Exeter EX4 4QL, UK

³ Department of Astronomy, University of Michigan, Ann Arbor, MI 48109, USA

⁴ University of Colorado Boulder, Boulder, CO 80303, USA

⁵ Department of Physics and Astronomy, Georgia State University, Atlanta, GA, USA

⁶ Infrared Processing and Analysis Center, California Institute of Technology, Pasadena, CA, 91125, USA

⁷ Mount Wilson Observatory, The CHARA Array of Georgia State University, Mount Wilson, CA 91023, USA

⁸ Universitäts-Sternwarte München, Ludwig-Maximilians-Universität, Scheinerstr. 1, D-81679, München, Germany

The aforementioned observational techniques (direct imaging and radio interferometry) can not easily probe the very inner disk regions (<5 au from the host star) where most of the detected exoplanets are located. Infrared interferometry, however, is able to reach an angular resolution of ~ 1 mas and therefore to probe the first astronomical unit around a young star at a distance of few hundreds parsecs.

We here present a high angular resolution observational campaign on the transition disk surrounding HD179218. This campaign involving seven different instruments consists in polarimetric direct imaging in the visible, aperture masking observations in the near-infrared and long-baseline interferometric observations in the near and mid-infrared. The target is a group I disk located at a distance of 293 pc (Bailer-Jones et al. 2018). It has a high ionisation fraction of the PAH features (Seok & Li 2017) and the disk cavity was deduced from ^{12}CO and ^{13}CO ro-vibrational emission. Previous long-baseline interferometric observations in the mid-infrared suggested the presence of a gap (Fedele et al. 2008). Finally, it is the most extended object in the near-infrared long-baseline interferometric survey made with PIONIER at the VLTI (Lazareff et al. 2017). We will therefore first describe the observational campaign, then present the results of each individual observation and, finally, conclude with a global interpretation of the whole dataset.

2 The observations

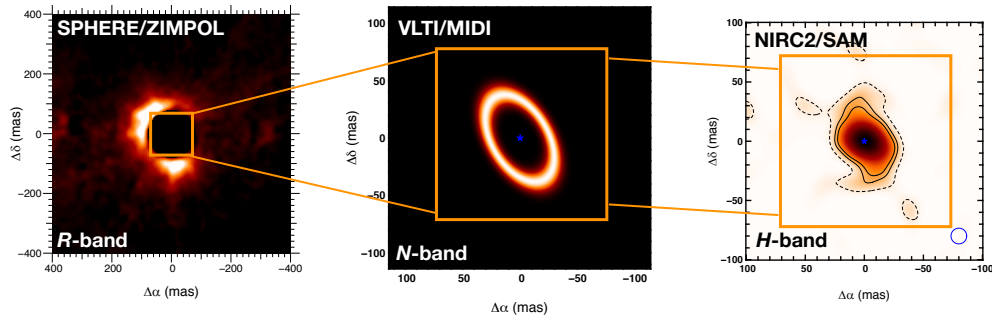


Fig. 1. Images of the circumstellar environment of HD179218 from the observing campaign. **Left:** Polarised intensity image with coronagraph in R -band from SPHERE/ZIMPOL. **Center:** image of the best-fit model to the archival visibility data from VLT/MIDI (between 8 and $12\mu\text{m}$). **Right:** Image reconstruction from aperture masking dataset from KECK/NIRC2 in the near infrared (at $1.65\mu\text{m}$).

2.1 SPHERE/ZIMPOL

We obtained SPHERE/ZIMPOL observations with the P2 mode with a coronagraph of 155 mas in diameter. Those observations are mainly tracing stellar light scattered onto the surface of the disk. There is an extended emission that can be reproduced by an off-centred Gaussian that has a full-width half-maximum (FWHM) of 252 ± 1 mas that translates into a size of ~ 75 au (Fig. 1). We do not see an inner cavity as this area is masked by the coronagraph. We can retrieve the disk orientation with an inclination (i) of $47.4^\circ \pm 0.3^\circ$ and a position angle (PA) of $24.8^\circ \pm 0.4^\circ$.

2.2 VLT/MIDI

We have also used archival data from the MIDI instrument (Menu et al. 2015) which is a two-telescope mid-infrared interferometer at the VLTI observing in the N -band ($8\text{--}12\mu\text{m}$). The visibility curve is looking like a Bessel function which is characteristic of a ring brightness distribution. We have fitted an inclined Gaussian ring to the data and found a ring radius of 42 ± 1 mas which translates into a physical radius of 12 au (Fig. 1). The inclination was found to be $i = 53^\circ \pm 6^\circ$ with a PA of $26^\circ \pm 6^\circ$ which is similar to what we found for the SPHERE/ZIMPOL observations.

2.3 KECK/NIRC2/SAM

The KECK/NIRC2 observations were obtained in the self aperture masking (SAM) mode in the H -band (at $1.65\mu\text{m}$). There is a clear squared visibility drop and a non-zero closure phase signal. We have first performed

an image reconstruction using MiRA (Thiébaud 2008) together with the SPARCO approach (Kluska et al. 2014) that enables to subtract the star from the image and reconstruct its environment only. The image reveals an extended emission from the star to about 40 mas in major-axis and 25 mas in the minor-axis (Fig. 1).

2.4 VLTI/PIONIER&AMBER

The VLTI observations were taken with PIONIER, a 4-beam interferometric instrument observing in H -band, and with AMBER in K -band ($2.2\mu\text{m}$). The closure phase signal is consistent with 0° (i.e. with a centrally symmetric brightness distribution). The squared visibility have the same level across the baselines (V^2 around 0.35 for PIONIER and 0.15 for AMBER). However, both instruments have several channels across their observing band (3 for PIONIER and 8 for AMBER) and there is a consistent slope of the V^2 with wavelength which is the so-called chromatic effect (Kluska et al. 2014). This effect is due to the difference of spectral index between the unresolved component (here, the star) and the extended component (the disk). This can be interpreted as a difference of a temperature between the hot star and the cold environment.

2.5 CHARA/CLIMB&CLASSIC

Finally, the CHARA long-baseline observatory allows to reach a baseline of 330 m in the near-infrared. We have obtained observations with CLIMB (3-beam interferometer) and CLASSIC (2-beam combiner) in the K -band. The squared visibility curve stays flat with the baseline length at a level of 0.15.

2.6 A geometric model reproducing the near-infrared interferometric data

Given the full interferometric dataset in the near-infrared we have fitted to it a Gaussian model with a star. The Gaussian FWHM is of 51 ± 2 mas which translates to about 10 au, which is smaller than the ring radius in the mid-infrared. The Gaussian has an inclination of $55^\circ\pm 3^\circ$ and a PA of $26^\circ\pm 3^\circ$. Those orientation are in accordance with mid-infrared and visible observations. The temperature of the near-infrared circumstellar emission is $T = 1440 \pm 30$ K.

3 The big picture

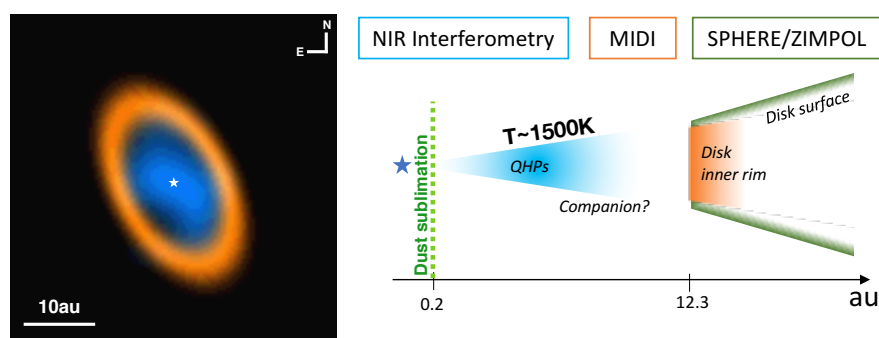


Fig. 2. A global view synthesising all our observations. **Left:** Composite image with mid-infrared emission in orange and near-infrared emission in blue. **Right:** Sketch of the emission seen by different instruments. The near-infrared emission is located inside the disk rim seen in mid-infrared, but is far more extended than the theoretical dust sublimation radius.

Finally, we can put all these high angular resolution observations to build one global picture. First, we have notified that the orientation (inclination and PA) of the extended emission is similar for all the observations, confirming that the same entity is observed, namely a disk with an inclination of $\sim 50^\circ$ and a PA of $\sim 25^\circ$.

The scattered light traces the disk surface behind the disk inner rim whereas the thermal infrared emission traces the disk inner rim which is at ~ 12 au. However, the near-infrared emission is located inside this inner rim as it has a FWHM of ~ 10 au. The temperature of this near-infrared emission is about 1500 K which is close to the dust sublimation temperature. This is not surprising as around young stars, the near-infrared emission is known to trace the dust sublimation radius (Monnier & Millan-Gabet 2002; Monnier et al. 2005; Lazareff et al.

2017). Nevertheless, the theoretical radius of dust sublimation is located at ~ 0.2 au, which is 50 times smaller than the observed size (Fig. 2). This points towards a special emission mechanism in this object.

Given the strong presence of PAHs, it is likely that this emission comes from quantum heated particles present inside the dust rim, as suggested by Klarmann et al. (2017). Those particles could be PAHs that are super heated by high energy photons from the central star. The last question is the origin of the disk inner rim that is not at the theoretical dust sublimation radius. It could be due to a yet unseen companion (our observations set an upper limit of $0.34 M_{\odot}$) or to the evolutionary state of the disk itself that could have accreted its inner rim, revealing the dust in the gap to high energy photons, and in the very early process of dissipating the rest of the disk.

4 Conclusions

The high angular resolution campaign with different instruments operating at different spatial scales and wavelengths enabled us to work out a global picture of the disk structure that would not have been possible with observations of one or two instruments alone. The disk structure of HD179218 is special not showing signs for an inner rim at the dust sublimation temperature but, instead, emission from quantum heated dust particles inside the disk hole. The disk itself seems to start at 12 au. This gap is either caused by a yet undetected planet or by photoevaporation where the inner disk was accreted onto the central stars and the rest of the disk (and particles in the disk hole) are exposed to stellar high-energy photons.

It would be interesting to follow-up this target with additional observations within the disk hole in the search for a companion and model the whole system with radiative transfer model including quantum heated particles.

We would like to thank the organisers of the S09 session and the LOC for organising this very nice SF2A meeting in Nice. The authors acknowledge support from a Marie Skłodowska-Curie CIG grant (Grant No. 618910), Philip Leverhulme Prize (PLP-2013-110), STFC Rutherford Fellowship (ST/J004030/1), and ERC Starting Grant (Grant Agreement No. 639889). A.A. and J.D.M. acknowledge support from NSF AAG 1311698. The authors wish to recognize and acknowledge the very significant cultural role and reverence that the summit of MaunaKea has always had within the indigenous Hawaiian community. We are most fortunate to have the opportunity to conduct observations from this mountain. This work was supported by a NASA Keck PI Data Award, administered by the NASA Exoplanet Science Institute (PID 69/2013B.N104N2). Data presented herein were obtained at the W. M. Keck Observatory from telescope time allocated to NASA through the agency's scientific partnership with the California Institute of Technology and the University of California. The Observatory was made possible by the generous financial support of the W. M. Keck Foundation. This work is based in part upon observations obtained with the Georgia State University (GSU) Center for High Angular Resolution Astronomy Array at Mount Wilson Observatory. The CHARA Array is supported by the NSF under Grant No. AST-1211929. Institutional support has been provided from the GSU College of Arts and Sciences and the GSU Office of the Vice President for Research and Economic Development. This research has made use of the SIMBAD database and the VizieR catalog access tool, operated at CDS, Strasbourg, France.

References

- Alexander, R., Pascucci, I., Andrews, S., Armitage, P., & Cieza, L. 2014, in *Protostars and Planets VI*, ed. H. Beuther, R. S. Klessen, C. P. Dullemond, & T. Henning, 475
- Andrews, S. M., Huang, J., Pérez, L. M., et al. 2018, *The Astrophysical Journal*, 869, L41
- Avenhaus, H., Quanz, S. P., Garufi, A., et al. 2018, *The Astrophysical Journal*, 863, 44
- Bailer-Jones, C. A. L., Rybizki, J., Founesneau, M., Mantelet, G., & Andrae, R. 2018, *The Astronomical Journal*, 156, 58
- Fedele, D., van den Ancker, M. E., Acke, B., et al. 2008, *A&A*, 491, 809
- Herbig, G. H. 1960, *The Astrophysical Journal Supplement Series*, 4, 337
- Klarmann, L., Benisty, M., Min, M., et al. 2017, *A&A*, 599, A80
- Kluska, J., Malbet, F., Berger, J.-P., et al. 2014, *A&A*, 564, A80
- Lazareff, B., Berger, J. P., Kluska, J., et al. 2017, *Astronomy and Astrophysics*, 599, A85
- Maaskant, K. M., Honda, M., Waters, L. B. F. M., et al. 2013, *A&A*, 555, A64
- Meeus, G., Waters, L. B. F. M., Bouwman, J., et al. 2001, *A&A*, 365, 476
- Menu, J., van Boekel, R., Henning, T., et al. 2015, *A&A*, 581, A107
- Monnier, J. D. & Millan-Gabet, R. 2002, *ApJ*, 579, 694
- Monnier, J. D., Millan-Gabet, R., Billmeier, R., et al. 2005, *ApJ*, 624, 832
- Seok, J. Y. & Li, A. 2017, *ApJ*, 835, 291
- Stolker, T., Sitko, M., Lazareff, B., et al. 2017, *The Astrophysical Journal*, 849, 143
- Thiébaud, E. 2008, in *Society of Photo-Optical Instrumentation Engineers (SPIE) Conference Series*, Vol. 7013, Society of Photo-Optical Instrumentation Engineers (SPIE) Conference Series, 1